The Climate Sensitivity and Its Components Diagnosed from Earth Radiation Budget Data

PIERS M. DE F. FORSTER

Department of Meteorology, University of Reading, Reading, United Kingdom

JONATHAN M. GREGORY

Centre for Global Atmospheric Modelling, Department of Meteorology, University of Reading, Reading, and Hadley Centre, Met Office, Exeter, United Kingdom

(Manuscript received 4 February 2005, in final form 5 June 2005)

ABSTRACT

One of the major uncertainties in the ability to predict future climate change, and hence its impacts, is the lack of knowledge of the earth's climate sensitivity. Here, data are combined from the 1985–96 Earth Radiation Budget Experiment (ERBE) with surface temperature change information and estimates of radiative forcing to diagnose the climate sensitivity. Importantly, the estimate is completely independent of climate model results. A climate feedback parameter of 2.3 ± 1.4 W m^{-2} K^{-1} is found. This corresponds to a 1.0–4.1-K range for the equilibrium warming due to a doubling of carbon dioxide (assuming Gaussian errors in observable parameters, which is approximately equivalent to a uniform "prior" in feedback parameter). The uncertainty range is due to a combination of the short time period for the analysis as well as uncertainties in the surface temperature time series and radiative forcing time series, mostly the former. Radiative forcings may not all be fully accounted for; however, an argument is presented that the estimate of climate sensitivity is still likely to be representative of longer-term climate change. The methodology can be used to 1) retrieve shortwave and longwave components of climate feedback and 2) suggest clear-sky and cloud feedback terms. There is preliminary evidence of a neutral or even negative longwave feedback in the observations, suggesting that current climate models may not be representing some processes correctly if they give a net positive longwave feedback.

1. Climate sensitivity

In 1990 the Intergovernmental Panel on Climate Change (IPCC) suggested a range of 1.5–4.5 K for the global surface equilibrium temperature increase associated with a doubling of CO_2 (Houghton et al. 1990). Since then, despite a massive improvement in models and in our understanding of the mechanisms of climate change, the uncertainty in our projections of temperature change has stubbornly refused to narrow (Houghton et al. 2001). A significant part of this uncertainty is due to different cloud feedbacks between models, although differences in other feedbacks, such as water vapor, also play a role (Houghton et al. 1990; Cess et al. 1996; Colman 2003). Recently, there have been several efforts to try and narrow this range using a combination of observations and climate model data; however, the large uncertainties in climate sensitivity have, if anything, increased (Forest et al. 2002; Gregory et al. 2002; Harvey and Kaufmann 2002; Knutti et al. 2003). In particular, it has proved extremely difficult to rule out very high values of climate sensitivity using observations (Gregory et al. 2002).

There are many definitions of climate sensitivity in the literature. While the most quoted sensitivity is the equilibrium warming for $2 \times CO_2$ this is not necessarily the most useful, as differences in the CO_2 radiative forcing can be confused with differences in climate response, and ideally one would like to know the climate response to any forcing mechanism. In this work, we use a standard linear definition of climate sensitivity, which we state here, and go on to show how it can be derived from observational data.

Corresponding author address: Piers Forster, School of Earth and Environment, University of Leeds, Leeds LS2 9JT, United Kingdom.
E-mail: piers@env.leeds.ac.uk

A linear climate feedback parameter (Y) can be defined, where

$$Y = -\frac{\partial N}{\partial \Delta T_s}, \quad (1)$$

and where N is the net downward irradiance at the top-of-atmosphere (TOA) energy balance and ΔT_s is the surface temperature change.

Consider factors that *directly* affect the top-of-atmosphere flux (N):

$$N(F, \Delta T_s, X) = N_o + \frac{\partial N}{\partial \Delta F}\Delta F + \frac{\partial N}{\partial \Delta T_s}\Delta T_s + \frac{\partial N}{\partial \Delta X}\Delta X + \text{non-linear terms}, \quad (2)$$

where F is a surrogate parameter for *external* radiative forcing mechanisms and X represents all the other *internally driven* mechanisms that might affect N, which are not directly or indirectly related to surface temperature

As we are concerned with linear changes in N, we can set $N_o = 0$ and ignore the nonlinear terms. The term $(\partial N/\partial \Delta F)\,\Delta F$ is a radiative forcing term, which we chose to rewrite as Q:

$$N = Q - Y\Delta T_s + \frac{\partial N}{\partial \Delta X}\Delta X. \quad (3)$$

This equation includes a term $[(\partial N/\partial \Delta X)\,\Delta X]$ that allows N to vary independently of surface temperature. A similar equation was used by Gregory et al. (2004). If we regress $(Q-N)$ against ΔT_s, we should be able to obtain a value for Y.

The X terms are likely to contaminate the result for short datasets, but provided the X terms are uncorrelated to ΔT_s, the regression should give the correct value for Y, if the dataset is long enough.

The concept of radiative forcing relates this climate feedback parameter to the expected equilibrium surface warming (ΔT_{eq}) caused by a constant radiative forcing (Q_c; Houghton et al. 2001):

$$\Delta T_{eq} = Q_c/Y_{NET}. \quad (4)$$

If the radiative forcing (Q_c) is due to a doubling of carbon dioxide (approximately 3.7 W m^{-2}), then ΔT_{eq} is termed the *equilibrium climate sensitivity*. A smaller value of Y_{NET} leads to a larger equilibrium surface temperature change and corresponds to a larger equilibrium climate sensitivity. Models indicate that while most radiative forcing mechanisms have climate sensitivities that are within ~30% of that from carbon dioxide changes, some do not, such as absorbing aerosol and ozone changes (Hansen et al. 1997; Joshi et al. 2003). Also, for the same radiative forcing mechanism, a climate model's climate sensitivity can vary with time, and some climate feedbacks, such as certain cloud changes, may not be linear (Colman et al. 1997; Senior and Mitchell 2000; Gregory et al. 2004). Acknowledging these limitations, we search for a single value for Y_{NET} in observations, and return to discussion of its applicability later.

2. Method

For our approach we use Eq. (3) to diagnose the climate feedback parameter (Y_{NET}) from observed time series of N and ΔT_s. We estimate corresponding values for Q and then regress $Q-N$ against ΔT_s to find a value for Y_{NET} from the slope of the regression line (also see Gregory et al. 2004). We use either seasonal data (with the annual cycle removed) or annual averages. Importantly, with this method, Y_{NET} is only determined by *changes* in N, Q, and ΔT_s over the time period considered. Hence, we do not need to identify a base state of zero climate change. The methodology is applicable to: 1) an equilibrium nonforced situation, where Q would be constant and N is responding to internal variability in ΔT_s; 2) transient forced climate change situations, where N and ΔT_s are responding to a radiative forcing (Q); and 3) a combination of internal variability and forced climate change. Sources of absolute error can safely be ignored as they only affect the intercept of the regression line and not its slope; N in particular might be expected to have large absolute errors, being difficult to measure.

The best estimate of the equilibrium climate sensitivity and its uncertainty range are derived from the linear regression analyses. The choice of linear regression model has an important influence on results, since the scatter is quite large. For our analyses, we adopted a robust fitting technique, based on ordinary least squares (OLS) regression of $Q-N$ against ΔT_s (Feigelson and Babu 1992). Compared to other techniques this gave larger error estimates. For a number of reasons we believe that OLS methodology was the most appropriate choice of the regression model. Ordinary least squares regression will give a bias toward small Y values and high climate sensitivities; all the other linear regression models examined suggested less than a 2-K doubling for $2 \times CO_2$ (see appendix).

For the uncertainty analysis we assume, like Gregory et al. (2002), that errors in the observable parameters (N, Q, and ΔT_s) all have Gaussian distributions. In a Bayesian statistics framework, this is equivalent to assuming Gaussian observational errors and a uniform "prior" in each of the observables. Since the uncertainties in Q and N are much larger than in ΔT_s (a factor influencing our choice of regression model; see appendix), uncertainty in $Q-N$ is linearly related to uncertainty in Y, so our assumption is also approximately

equivalent to assuming a uniform prior in Y. Other studies (Forest et al. 2002; Knutti et al. 2003) have assumed a prior that is uniformly distributed in equilibrium climate sensitivity, which is proportional to $1/Y$. Compared with our prior, theirs emphasizes the higher values of equilibrium climate sensitivity. We believe our choice is more appropriate for our analysis and input data, but it has the result that our range of climate sensitivity lies lower. Differences in priors should be taken into account when comparing quoted ranges of possible temperature change.

3. Data

a. Net energy imbalance (N)

For this work we take N to be the net flux imbalance at the top of the atmosphere (positive downward) measured by instruments on the Earth Radiation Budget Satellite (*ERBS*); we use data from the 15 yr of wide-field-of-view (WFOV) data and the shorter ~5 yr dataset from the scanning radiometer. These instruments measure radiation between 60°S and 60°N. The WFOV instrument uses two cavity radiometers to measure the absorbed solar radiation and the outgoing longwave radiation (OLR); the scanning instrument measures shortwave (SW) and longwave (LW) radiances with a thermistor bolometer (Wielicki et al. 2002). As a result of battery problems, there are several gaps in the data, especially during 1993, and for these reasons we do not use data from 1993 or after 1997 for computing annual averages. Our data are essentially the same as the datasets presented in Wielicki et al. (2002), except we have additionally applied a correction to the WFOV data for the decay in the satellite's orbit (T. M. Wong 2005, personal communication). This correction reduces the positive trend in OLR and increases the positive trend in absorbed solar radiation. The annual averaged anomalies used in this study from the WFOV instrument are shown in Fig. 1b. These data arguably represent the best observations we have for N and relative calibration in SW and LW fluxes are expected to be better than 0.5 W m^{-2} (for decadal timescale changes) and even better than this on interannual time scales (Wielicki et al. 2002). The changes we observe in the data are considerably larger than this (see Fig. 1b).

b. Surface temperature (ΔT_s)

We use two global surface temperature anomaly datasets; one from the Goddard Institute for Space Studies (GISS; Hansen et al. 1999) and the other from the Hadley Centre and University of East Anglia's Climate Research Unit (HADCRU) (Jones et al. 1999). Their anomalies are similar for the 1985–97 period (Fig. 1a). However, the two surface temperature time series shown give quite different changes between 1996 and 1997. As our approach is dependant on stable time series of robust data, 1997 was excluded from subsequent analysis.

c. Radiative forcing (Q)

Radiative forcing time series were obtained from various sources (Sato et al. 1993; Myhre et al. 2001; Hansen et al. 2002). We found that volcanic and well-mixed greenhouse gas radiative forcings played the most important role in determining Y_{NET}; changes in total solar irradiance also had some effect, but these values could be derived directly from the ERBS instruments, which largely eliminated them as a source of uncertainty. Time series of the important datasets are shown in Fig. 1c. The tropospheric aerosol direct and indirect radiative forcings were found not to impact our regression. Despite potentially large absolute errors in these forcings, their impact on our analysis is likely to be small, as the tropospheric aerosol forcing in the datasets analyzed *changed* very little over 1985–96 (Myhre et al. 2001). However, we acknowledge that any undiagnosed change in aerosol radiative forcing could have significant effects on our shortwave results. Over this relatively short time period any undiagnosed forcing changes would likely be uncorrelated with global mean surface temperature changes; these forcings would therefore increase the uncertainty, or noise, in the analysis, rather than lead to systematic errors in Y. The forcing that had by far the largest impact on the regression was volcanism and, in particular, the eruption of Mt. Pinatubo in 1991. For this study, we used SW and LW volcanic forcing estimates from several sources (derived from data outlined in Myhre et al. 2001; Sato et al. 1993). This volcanic forcing may be in error by as much as 30% (Houghton et al. 2001); the impact of this uncertainty on the results is discussed in the results (and in Table 3).

As the ERBS instruments measured SW and LW components of the energy budget separately, the shortwave climate feedback parameter (Y_{SW}) and longwave climate feedback parameter (Y_{LW}) could also be found. To do this, we separately considered SW or LW components of Q and N in Eq. (1) for the regression analysis. For the scanning instrument, we were able to further subdivide N into clear- and cloudy-sky components and use these to find corresponding Y values. For the regression of $Q-N$ versus ΔT_s an appropriate Q, representative of the N being measured, needed to be estimated. Therefore, to derive Y_{SW} and Y_{LW} we had to

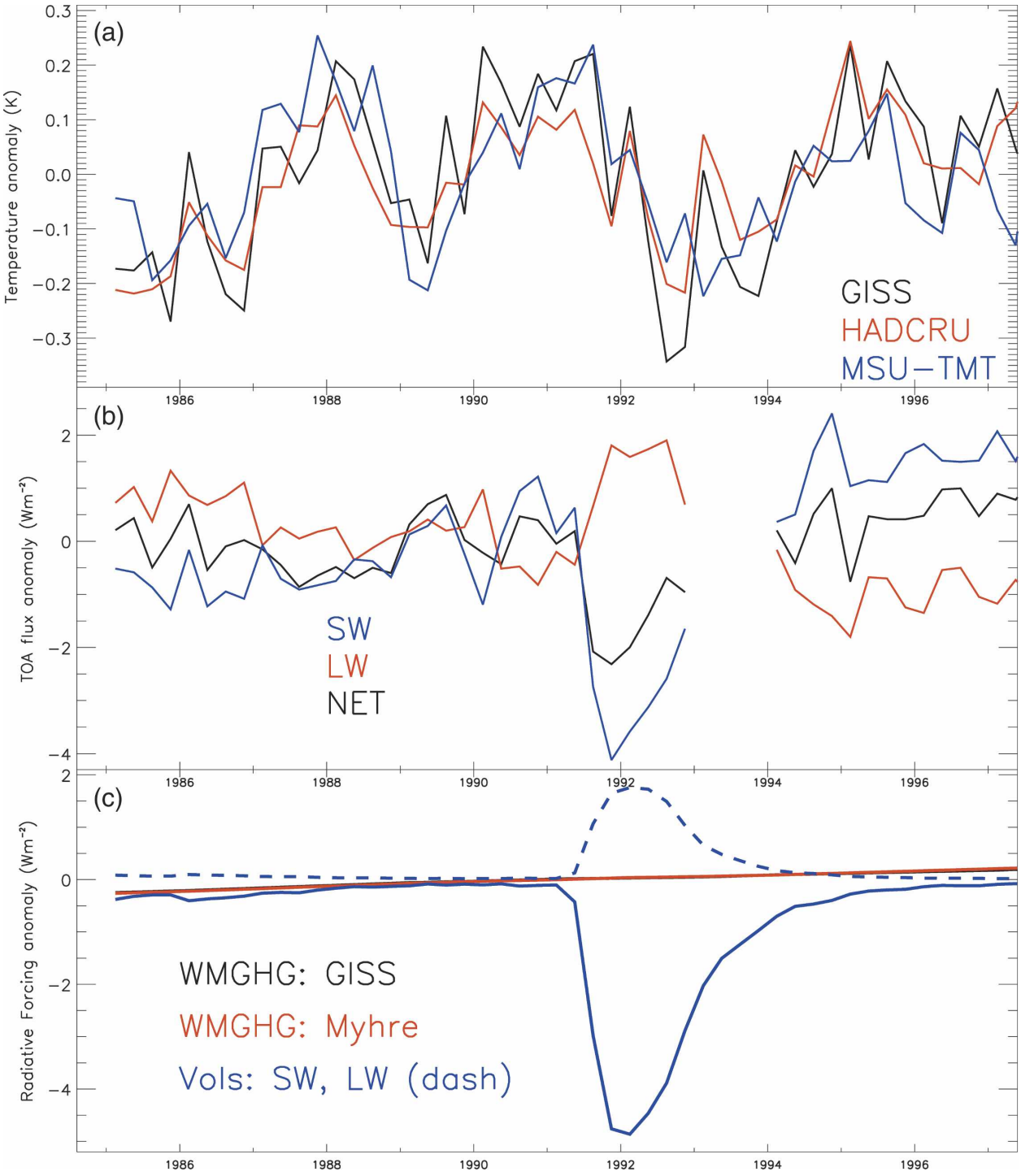

FIG. 1. The 1985–97 globally averaged seasonal anomalies in (a) surface temperature (HADCRU, GISS) and midtropospheric temperature (MSU-TMT), (b) ERBE WFOV *N* data, and (c) well-mixed greenhouse gas and volcanic radiative forcing. The seasonal cycle has been removed from these datasets. ERBE *N* values are all measured positive downward, and 1993 data are not shown due to missing data in the ERBE record.

TABLE 1. For different time periods the table shows the Y_{SW}, Y_{LW}, and Y_{NET} values derived from the WFOV instrument. A 95% uncertainty and the correlation of $Q-N$ vs ΔT_s are also presented. Data are shown for the two surface temperature anomalies (HADCRU and GISS). These data use the GISS well-mixed greenhouse gas forcing. Results are shown for seasonal and annual anomalies, with the seasonal cycle removed from the seasonal data.

	SW			LW			NET		
Year range	Y W m^{-2} K^{-1}	95% error W m^{-2} K^{-1}	Correlation	Y W m^{-2} K^{-1}	95% error W m^{-2} K^{-1}	Correlation	Y W m^{-2} K^{-1}	95% error W m^{-2} K^{-1}	Correlation
				GISS (ΔT_s)					
1985–90	−1.4	2.5	−0.51	3.6	0.9	0.97	2.4	2.2	0.71
1985–96 (no 1993)	−1.6	3.3	−0.23	3.8	2.4	0.62	2.3	1.3	0.66
1985–90 (seasonal)	−1.4	1.5	−0.34	2.6	1.3	0.67	1.4	0.8	0.40
1985–96 (seasonal)	−1.3	1.6	−0.19	2.7	1.2	0.51	1.5	0.7	0.43
Pinatubo 1991–92 (seasonal)	1.1	1.0	0.57	0.9	0.9	0.62	2.1	1.3	0.74
				HADCRU (ΔT_s)					
1985–90	−1.6	3.5	−0.50	4.4	1.5	0.95	2.9	3.2	0.70
1985–96 (no 1993)	−3.3	3.7	−0.41	5.7	0.2	0.75	2.5	1.8	0.54
1985–90 (seasonal)	−1.2	2.0	−0.22	3.3	1.6	0.64	2.4	1.1	0.51
1985–96 (seasonal)	−2.6	2.0	−0.32	4.4	1.4	0.62	1.8	1.1	0.37
Pinatubo 1991–92 (seasonal)	1.4	2.0	0.41	1.4	1.7	0.57	2.9	2.4	0.60

split radiative forcing into SW and LW components. For the cloudy case where N_{cloud} is taken to be $N-N_{clear}$ we set Q to zero. This assumes that there is no difference between the clear-sky and all-sky radiative forcing terms. In practice, over the short 5-yr time period where the scanner data were available, Q uncertainties had little impact on the derived Y values.

4. Results

For several time periods, we present values for the total climate feedback parameter (Y_{NET}) and its components. For the *ERBS* WFOV instrument, we divide the record into the pre-Pinatubo period (1985–90), the Pinatubo years (1991–92), and the 1985–96 period; 1993 is missing in the ERBE record. Table 1 gives the results of the regression analyses, using both annual averages and seasonal data (with the annual cycle removed); it also compares the results from using the two surface temperature datasets. Corresponding figures to several of these regressions are shown in Figs. 2 and 3. Figure 4 summarizes the overall findings for the annual results of the WFOV instrument. Consistent with the lower correlations, seasonal climate feedback parameters are slightly smaller in magnitude than the feedback parameters derived from annual averages, although they agree to within their respective uncertainty estimates. Results derived from annual averages typically have the highest correlations. Table 2 and Fig. 5 show the results of the scanning instrument analyses, which are summarized in Fig. 6.

The results show that the linear model of climate sensitivity adopted works well in the longwave, and we are able to quantify Y_{NET} quite well and Y_{LW} values better. For Y_{SW} the simple model does not work as well, but we are still able to usually determine a sign. Figure 4 shows that over both the pre-Pinatubo period and the 1985–96 record we find that a Y_{LW} of ~4 W m^{-2} K^{-1} is partly offset by a likely negative Y_{SW}, to give a Y_{NET} of ~2.0 W m^{-2} K^{-1}. Several climate models exhibit a similar "NET" positive feedback (Houghton et al. 2001). The NET climate feedback derived from the Pinatubo response is similar, but its LW and SW components are very different. Uncertainties in the radiative forcing (see below) cannot account for these differences, so these results indicate that the Pinatubo year's climate response is not the same as the longer-term response. The 1985–89 results from the scanning instrument agree well with those from the WFOV instrument (Table 2). Although errors in the regression are much larger, the scanning instrument also hints at the clear- and cloudy-sky feedbacks.

5. Uncertainties in deriving *Y* values

The 95% uncertainties for Y, presented in the tables, are purely statistical and are from the straight-line fits. However, we also analyzed the effects of using different temperature and/or radiative forcing datasets (Table 1 and Table 2), and compared results from annually averaged data with those from seasonal data (Table 1).

In the LW, $Q-N$ values are well correlated to ΔT_s values, especially for the 1985–90 period, where correlations are larger than 0.95 for the annual averages and the regression gives a near-perfect straight line for Y_{LW}. For all the time periods analyzed, both Y_{LW} and Y_{NET}

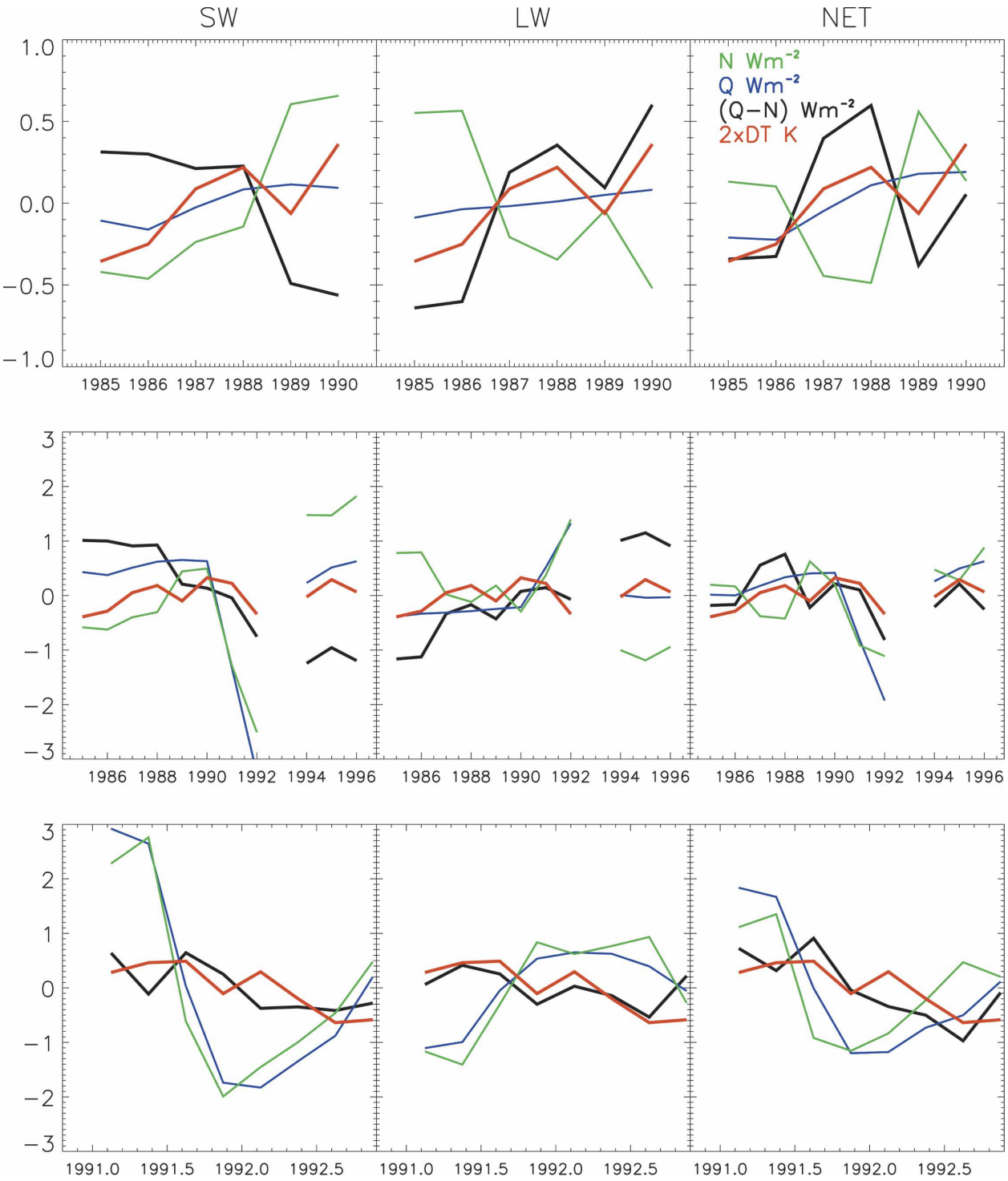

FIG. 2. Data used to derive *Y* values from WFOV data. Shown are the SW, LW, and NET flux anomalies and the surface temperature anomalies (multiplied by 2 for scaling). GISS surface temperature and well-mixed greenhouse gas forcing datasets are employed. Data are for (top) 1985–90 annual data, (middle) 1985–96 annual data, and (bottom) and 1991–92 seasonal data.

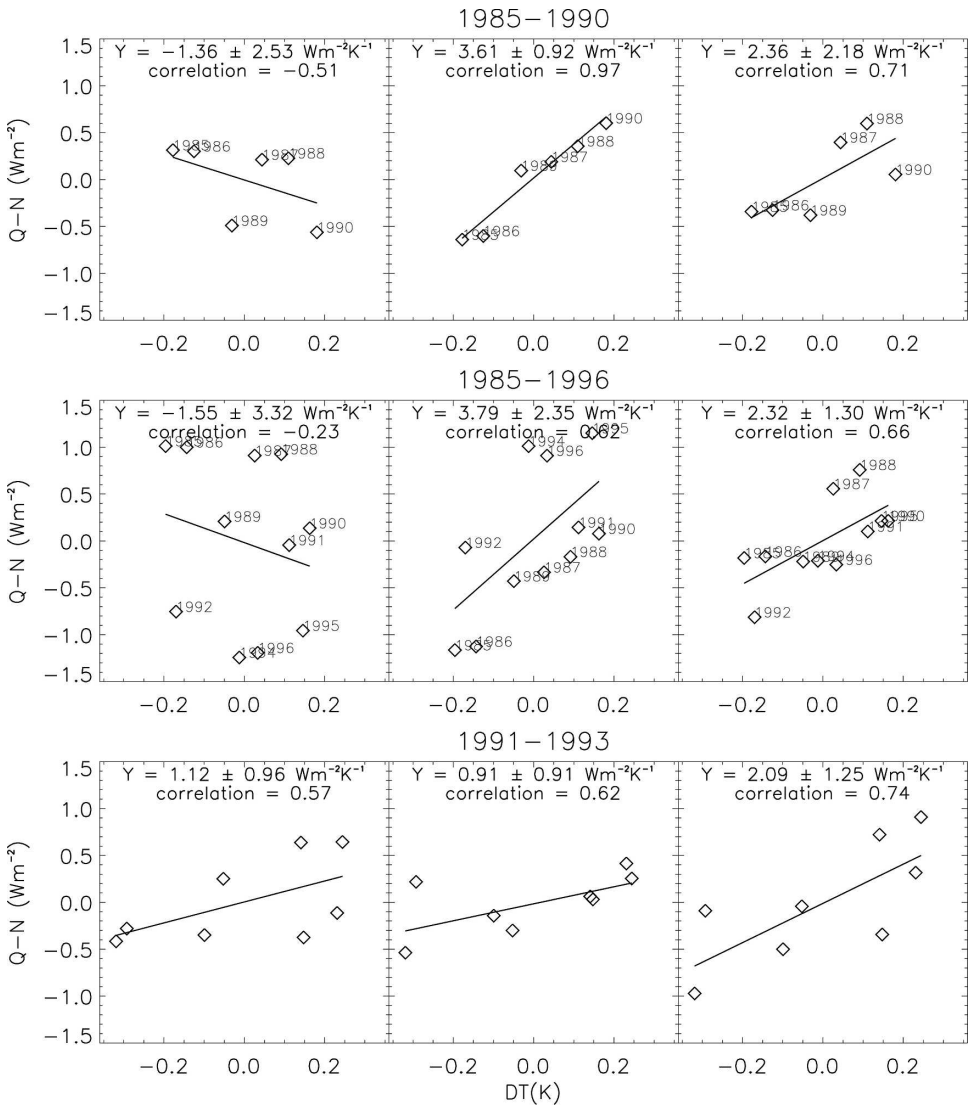

FIG. 3. Robust OLS linear regression of $Q-N$ vs ΔT_s from the data shown in Fig. 2. A Y value, with 95% uncertainty, and the correlation of $Q-N$ vs ΔT_s are also shown. GISS surface temperature and well-mixed greenhouse gas forcing datasets are employed. Regressions are for (top) 1985–90 annual data, (middle) 1985–96 annual data, and (bottom) 1991–92 seasonal data.

are reasonably well constrained by the regression analysis and correlations of annually averaged data are almost always above 0.6. The regression analysis does not work as well for deriving Y_{SW}; uncertainties are larger and correlations smaller, compared with those for Y_{LW} and Y_{NET}. Although its correlations are similar, the HADCRU surface temperature dataset gives higher Y_{LW} values than the GISS dataset. However, again, these differences are no larger than the 95% errors in the regression analysis. Annual Y_{NET} values for 1985–96 calculated with the two datasets differed by 0.2 W m^{-2} K^{-1}. For the summary in Figs. 4 and 6 the results from the analysis using the GISS surface temperature and forcing datasets are used as these often had higher correlations and smaller errors than found when using other analyses.

Table 3 analyzes how uncertainty in the radiative forcing term affects the derived Y_{NET} values. The volcanic forcing and the well-mixed greenhouse gas forcing (WMGHG) both play a role in determining Y values, and results become largely meaningless if either forcing is ignored. However, the two estimates of WMGHG forcing are very similar, so uncertainty in this forcing has a small effect on Y (0.1 W m^{-2} K^{-1}). In addition, we also examined the effect of including a 10% uncertainty estimate in the WMGHG forcing (Houghton et al. 2001); this also added 0.1 W m^{-2} K^{-1} to the overall uncertainty estimate. Varying the magni-

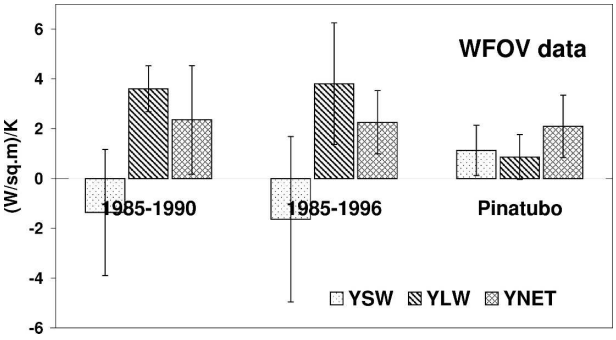

FIG. 4. Values of Y_{SW}, Y_{LW}, and Y_{NET} and their 95% uncertainties (vertical lines) from ERBE WFOV data. Annual values derived for the GISS surface temperature dataset are used.

tude of the volcanic radiative forcing by its suggested uncertainty of 30% (Houghton et al. 2001) changed Y_{NET} values by 0.5 W m^{-2} K^{-1}. Over the 1991–92 time frame of the major Pinatubo climate response, the forcing term plays a larger role; but, even here, uncertainty in the forcing only varied Y_{SW} by 1.0 W m^{-2} K^{-1} and Y_{LW} by 0.5 W m^{-2} K^{-1}. We can therefore conclude that, provided we are not ignoring an important forcing term, uncertainties in radiative forcing ought not to have had a major impact on the derived Y values. If there are undiagnosed aerosol changes, they would impact our analysis. However, as the temperature changes over this time period are far from being a monotonic increase (Fig. 1), it would hopefully be unlikely that any undiagnosed forcing would correlate with ΔT_s. If these forcings were uncorrelated with ΔT_s, aerosol would be unlikely to alter the slope of the regression; rather they would make the regression noisier. Some of the noise in the Y_{SW} regression could easily be the result of this undiagnosed forcing. However, experiments with the Third Hadley Centre Coupled Ocean–Atmosphere GCM (HadCM3), in which all the forcings were known (Gregory et al. 2004), also found a noisier Y_{SW}. It is likely that shortwave cloud feedback processes also account for at least part of this noise (also see section 7). If, however, aerosol was correlated with ΔT_s (such as could conceivably be the case with forest fires), it could have a major impact, especially on our estimate of Y_{SW}.

To estimate the complete error in our analysis of Y we also need to include the likely error introduced by uncertainties in the ERBE time series. Over 1985–96 the total change in $Q-N$ is about 2–3 W m^{-2} (Fig. 1), which can be compared to a suggested interdecadal calibration error of less than 0.5 W m^{-2} (Wielicki et al. 2002). A change in the N of 0.5 W m^{-2} would significantly alter the results. However, these errors would not necessarily correlate with ΔT_s, so the fact that the regression gives any meaningful results at all, and sometimes very good straight line fits, indicates that the ERBE data may be reliable. Similar analyses with other available datasets for N produced little or no meaningful result. The N values were also estimated using 1981–87 *Nimbus-7* data (Jacobowitz et al. 1984), 1950–2000 ocean heat uptake data (Levitus et al. 2000), and a 1983–2000 dataset derived from several satellite instruments (Zhang et al. 2004). Several time periods were considered. For the *Nimbus-7* analysis, although uncertainties are much larger, correlations were found to be around 0.5 for Y_{NET} and Y_{LW}, and the derived Y values agreed well with those from the ERBE data. For the other datasets, $Q-N$ and ΔT_s were always uncorrelated and no significant relationships were found. Using the WFOV data without their latest orbital decay corrections also gave an indication of how uncertainty in N affected our results. For the 1985–96 time period, the uncorrected data, compared to the results in Table 1, gave a much higher value for Y_{LW} (but the correlations were ~0.2 smaller). This resulted in a Y_{NET} of around 4.0 W m^{-2} K^{-1}, which would correspond to only a 1-K warming for a doubling of carbon dioxide.

The errors in ERBE that would have the largest affect on our derived Y values are those caused by long-term calibration drift; in these cases a correlation would remain. The data used in this study have had latest correction data applied; using the uncorrected data would increase Y_{NET} by over 50%. For the summarized

TABLE 2. The seasonally averaged Y_{SW}, Y_{LW}, and Y_{NET} values derived from scanner and WFOV data for 1985–89. The table also shows the 95% uncertainty in Y and the correlation of $Q-N$ vs ΔT_s. For the scanner data, Y is also separated into clear and cloudy scenes. The GISS surface temperature anomaly and well-mixed greenhouse gas forcing are employed. The results with the HADCRU surface temperature dataset and/or GISS radiative forcing dataset are very similar.

	SW			LW			NET		
1985–89 seasonal analysis	Y W m^{-2} K^{-1}	95% error W m^{-2} K^{-1}	Correlation	Y W m^{-2} K^{-1}	95% error W m^{-2} K^{-1}	Correlation	Y W m^{-2} K^{-1}	95% error W m^{-2} K^{-1}	Correlation
Type of measurement									
WFOV	−1.1	1.3	−0.32	2.6	0.9	0.76	1.7	1.2	0.42
Scanner	−0.3	1.8	−0.06	2.6	1.3	0.56	2.4	1.3	0.55
Scanner (clear sky)	1.1	0.7	0.50	1.0	1.6	0.24	2.2	1.6	0.46
Scanner (clouds)	−1.4	1.6	−0.32	1.6	1.6	0.31	0.2	1.4	0.04

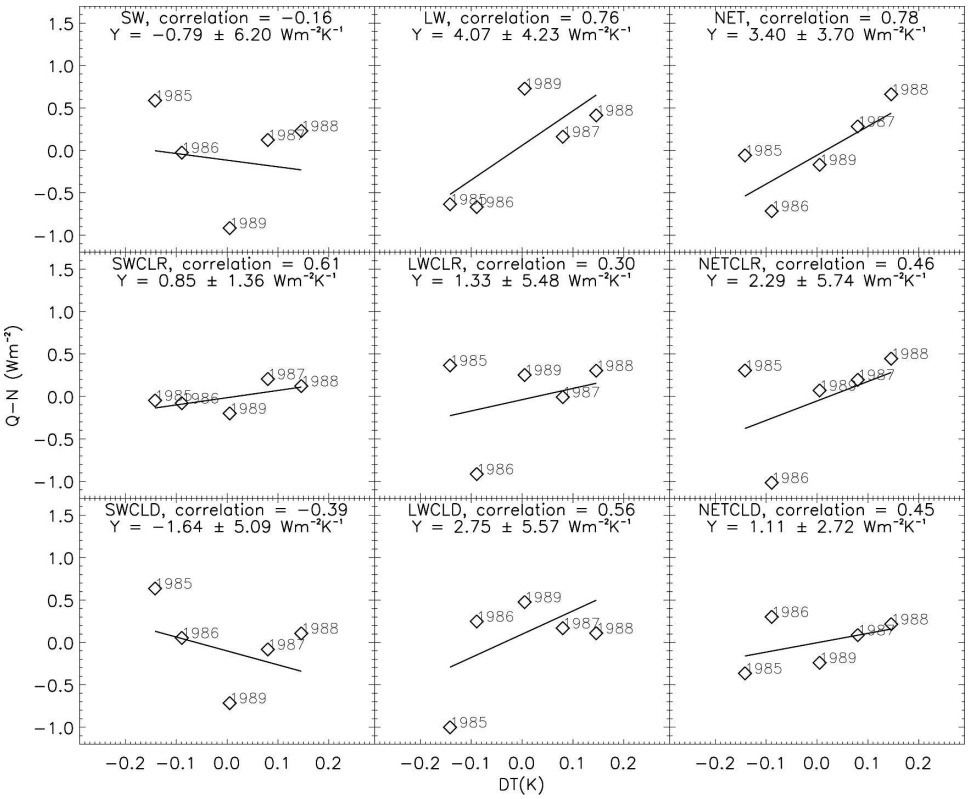

FIG. 5. Values of Y derived from annually averaged 1985–89 scanner data. Panels show the linear regression of $Q-N$ vs ΔT_s. A Y value, with 95% uncertainty, and the correlation of $Q-N$ vs ΔT_s are also shown. (top) T Total Y_{SW}, Y_{LW}, and Y_{NET} values; (middle), (bottom) the clear- and cloudy-sky components of these Y values, respectively. GISS surface temperature and well-mixed greenhouse gas forcing datasets are employed.

Y values and their uncertainties, presented in Figs. 4 and 6 and in the conclusions, we assume that the corrected ERBE time series are *perfect* apart from an unknown constant offset.

To obtain the overall uncertainty estimate presented in the abstract and conclusions, we took the central best estimate, with the GISS dataset and used its regression uncertainty range. We then added surface temperature and radiative forcing uncertainties (discussed above), assuming they are independent of each other. This gave an overall uncertainty estimate for Y_{NET} of 2.3 ± 1.4 W m^{-2} K^{-1}. This uncertainty range does not account for uncertainty in the ERBE time series (N). We used the GISS central estimate and its regression uncertainty, as these data had the highest correlations. Reasons for using the highest correlation to select the central value are that it may suggest that this dataset is more reliable, and the regression will have the smallest bias in the OLS slope.

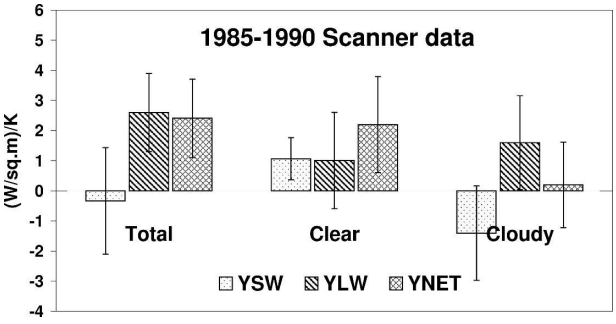

FIG. 6. Same as in Fig. 5, but from ERBE scanner data. Results are also shown for the clear-sky and cloudy values. Seasonal values derived for the GISS surface temperature datasets are used.

6. Applicability of results for long-term climate change

Here we ask two questions about the applicability of the results for determining future climate change.

a. How representative is Y_{NET} of the climate feedback from CO_2-induced global warming?

Model results indicate that Y varies between different forcing mechanisms, especially ones with very different patterns of surface and vertical temperature

TABLE 3. Y_{NET} values derived from WFOV data, using different radiative forcings. Two WMGHG forcings are used [Hansen et al. (2002): GISS and Myhre et al. (2001): MYHRE]. The volcanic forcing from Sato et al. (1993; SATO) is also varied. The table also shows the 95% uncertainty in Y_{NET} and the correlation of $Q-N$ vs ΔT_s. The GISS surface temperature anomaly is used. Y_{NET} values are shown as they are affected more by Q than either Y_{SW} or Y_{LW}, this is because Y_{NET} is essentially as residual between a negative Y_{SW} and positive Y_{LW}.

1985–96 analysis, GISS (ΔT_s) Q series	NET		
	Y W m^{-2} K^{-1}	95% error W m^{-2} K^{-1}	Correlation
GISS(WMGHG), SATO (volcanic)	2.3	1.3	0.66
MYHRE(WMGHG), SATO (volcanic)	2.2	1.3	0.65
MYHRE(WMGHG), 0.7SATO (volcanic)	1.7	1.5	0.48
No WMGHG, SATO volcanic	1.0	2.5	0.12
MYHRE(WMGHG), no volcanic	0.4	3.1	0.06
No forcing	−0.4	3.1	−0.07

change (Hansen et al. 1997; Joshi et al. 2003). If our Y_{NET} value is derived from tropical temperature variability and El Niño, it could be unrepresentative of long-term climate change (Soden 1997; Houghton et al. 2001). Furthermore, it has also been suggested that subannual changes in temperature are often confined to the surface layer and that using such changes to diagnose climate feedback leads to an underestimate of the water vapor feedback (Hall and Manabe 1999). In addition, the ERBE instruments do not measure radiation poleward of 60°, so they may not adequately detect certain climate feedbacks, particularly the surface albedo feedback.

The years 1995 and 1985 span the range of global ΔT_s anomalies seen in the time series. Figure 7 shows that the change in surface temperature between these two years has a pattern that is a little like that of both the observed long-term surface temperature trends (e.g., Houghton et al. 2001, their Fig. 2.9d). Furthermore, Fig. 1 shows that the 1985–97 temperature changes are occurring throughout the troposphere, in a similar manner to that expected from long-term climate change. Therefore, we argue that the Y values we derive from the regression are likely to be representative of those due to longer-term climate change. In addition, using shorter time periods where the temperature changes may not be representative of longer-term climate change (such as 1991–92) gives distinctly different answers (Fig. 4). However, as it is likely that the observed temperature changes are a combination of variability (on different time scales) and forced climate change, with contributions from different forcing agents, there is still the possibility that such variability biases our result. For example, this variability could involve circulation responses that differ from those expected in a long-term climate change situation. Thus, our diagnosed climate sensitivity may also be a signature of this variability.

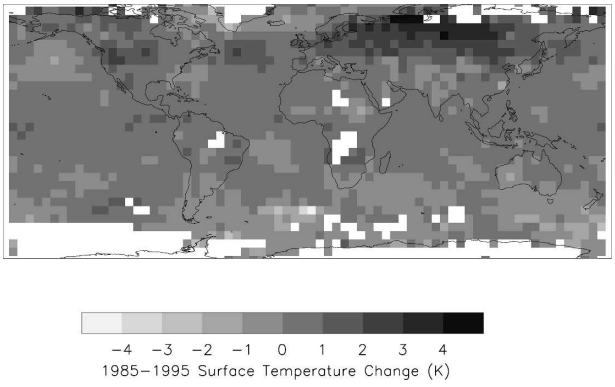

FIG. 7. The 1985–95 change in annually averaged surface temperature. Temperature anomalies are taken from HADCRU data.

Integrations from HadCM3 were also employed to test the regression technique. We analyzed data from a HadCM3 integration of 1860–2100 with historical greenhouse gas concentrations and future concentrations following the IFCC Scenario 1992a (IS92a; Legget et al. 1992). The result from the regression was $Y = 1.11 \pm 0.02$ W m^{-2} K^{-1}, which is much more precise than from the observations because the future radiative forcing and the resulting climate change are large, so the signal/noise is improved. Gregory et al. (2004) used the regression method of diagnosing climate sensitivity to compare its value in the coupled model (HadCM3) to that in the slab version of the same model. (The "slab" model uses a mixed layer ocean of 50-m depth with prescribed heat convergences rather than a 3D ocean GCM. Because the slab ocean heat capacity is relatively small, this kind of model is frequently used to diagnose equilibrium climate sensitivity.) They found the CO_2 climate sensitivity of the slab model to be slightly higher than in the first century of coupled model integrations, the latter being in agreement with our value above from the IS92a integration. If equilibrium and transient integrations give different Y values, the latter

is practically more relevant for projections of climate change in coming decades.

We then analyzed the years 1985–96 in an ensemble of four HadCM3 simulations of the twentieth century forced by both natural and anthropogenic factors (from Stott et al. 2000). The mean of the four Y values was 1.6 W m^{-2} K^{-1} and the standard deviation was 1.2 W m^{-2} K^{-1}, implying a standard error of estimate of 0.6 W m^{-2} K^{-1} on Y from the ensemble. The "true" value of 1.1 W m^{-2} K^{-1} lies within this interval of 1.6 ± 0.6 W m^{-2} K^{-1}, suggesting that the observed data should similarly give an estimate of the climate sensitivity relevant to projections in the real world. Moreover, the ensemble standard deviation of 1.2 W m^{-2} K^{-1} was similar to the typical uncertainty on the slope estimated from the regression procedure in the individual integrations; the mean of the regression uncertainties was 1.1 W m^{-2} K^{-1}, suggesting that the regression uncertainty from the observed data should give a good estimate of the accuracy of our Y value. In the model, excluding data poleward of 60° from calculations of global radiation made only a small difference to the Y value (reducing it to 1.5 ± 0.6 W m^{-2} K^{-1}), because the surface albedo term is not a dominant component of the total climate feedback (Colman 2003), and in the model much of the surface albedo feedback term comes from seasonal snow cover on the northern continents south of 60°N. Further discussion of differences between model and observations is outside the scope of this study.

b. *How good is the linear model of climate sensitivity?*

As well as data errors, poor correlations could also arise if different responses from different forcings were being observed in the same dataset. This is certainly the case for 1985–96, as we include the Pinatubo response, knowing its climate feedback to be different (Fig. 4). However, excluding 1991–92 only decreased uncertainties in the 1985–96 derived Y values by ~20% (not shown), which indicates that this issue is unlikely to be a major source of uncertainty in the regression. The linear model appears to work particularly well in the LW, but not as well in the SW (Figs. 2 and 3). This is also found to be the case in models, where the poorer fit in the SW has been attributed to nonlinear cloud effects (Colman et al. 1997). The scanner data support this hypothesis, as they reveal a better straight-line fit for clear-sky Y_{SW} value*s*, compared to cloudy Y_{SW} values. Another possibility is that internal variability in the climate system produces fluctuations in cloud cover, causing cloud forcings, especially in the shortwave, that will be seen in N and produce a lagged response in ΔT_s and cloud feedbacks. This mixture of forcing and feedback will degrade the correlation. Analysis of the HadCM3 control integration, which has no externally forced changes, supports this possibility. There is internally generated variability in TOA fluxes and ΔT_s; the clear-sky Y values are statistically consistent with the response to greenhouse gases, but the cloudy-sky response shows poor correlation.

7. Climate feedbacks

The Y values derived can be interpreted in terms of climate feedbacks. With no feedback, the earth behaves like a blackbody and we expect a $Y_{NET} = Y_{LW}$ response of roughly 3.3 W m^{-2} K^{-1} (Colman 2003). This Y value can be increased through negative feedbacks that make the climate response smaller [through Eq. (2)] or decreased by positive feedbacks that would make the climate response larger. For the long-term changes, a substantial positive SW feedback ($Y_{SW} < 0$) and a small negative LW feedback combine to decrease Y_{NET} and give an overall positive feedback of ~1.3 W m^{-2} K^{-1}.

Over the short 1985–90 time period, we appear to find a near neutral LW feedback (Y_{LW} is close to 3.3 W m^{-2} K^{-1}). This result is particularly interesting as most climate models exhibit a positive longwave feedback (Houghton et al. 2001). If our results are accurate, it could mean either that there is little or no positive water vapor feedback and a neutral cloud feedback or it could imply that the longwave cloud feedback is negative, offsetting the positive water vapor feedback. In contrast, during the Pinatubo years the longwave feedback is positive (~2.3 W m^{-2} K^{-1}). This value agrees both with estimates of the water vapor feedback diagnosed from observations over the same period and with that diagnosed from climate models (Soden et al. 2002; Forster and Collins 2004). Therefore, if the water vapor feedback is similar over the entire time period (which appears to be the case; see below), one might speculate that during the Pinatubo cooling the longwave cloud feedback is near to neutral, but over the full period it is negative. Differences in global feedbacks (and hence in Y) for different forcing agents could plausibly be caused by the differing geographical and seasonal distribution of the forcings concerned. Volcanic forcing, for instance, is principally in the shortwave and hence greater when insolation is high, whereas CO_2 forcing is in the longwave.

To try to answer some of these questions we can extend this analysis to other climate feedbacks with the scanner data for the 1985–90 period. Note that this discussion is somewhat speculative as errors in the regressions for the scanner data are large and the conclusions are particularly dependent on the ability of the ERBE algorithms to unambiguously separate clear and cloudy

scenes. This feedback analysis uses the cloud radiative forcing concept (Cess et al. 1996; Houghton et al. 2001). As a result of cloud masking of the noncloud feedback terms, feedbacks analyzed using cloud radiative forcing will be systematically different than those from partial radiative perturbations (Soden et al. 2004). Soden et al. found that in one climate model the cloud radiative forcing feedback was 0.3–0.4 W m^{-2} K^{-1} more negative than the actual cloud feedback. Likewise the clear-sky feedback analyzed employing cloud radiative forcing would be more positive than the actual clear-sky feedback.

a. Water vapor and lapse rate

Models and observations suggest a positive feedback of around 1.7 ± 0.4 W m^{-2} K^{-1} from water vapor and lapse rate changes (Colman 2003). When this number is subtracted from the blackbody Y_{LW} value, a clear-sky Y_{LW} of 1.6 W m^{-2} K^{-1} would result. Although it is one of the most uncertain of our Y retrievals, a similar number is seen for our clear-sky Y_{LW} results (Fig. 6).

b. Surface albedo

Models have a positive clear-sky albedo feedback ($Y_{SW} < 0$) of 0.4 ± 0.2 W m^{-2} K^{-1} (Colman 2003). However, our clear-sky SW results indicate a negative clear-sky albedo feedback. Applying the Soden et al. (2004) correction to our clear-sky feedback could mean that the actual clear-sky feedback is more negative still. The negative feedback we find may be due to the ERBE instruments being unresponsive to changes in N caused by the cryosphere, as they do not measure latitudes higher than 60°. However, climate model results indicated that this was unlikely to be the problem (see section 5b). Examining the pattern of N variations revealed no obvious large-scale regional pattern associated with a possible mechanism. However, it is also possible that feedback from thin clouds (for example) is being misinterpreted as a clear-sky feedback by the ERBE algorithms.

c. Clouds

The NET cloud feedback appears close to neutral in the scanner data; it is made up of components due to a positive SW feedback and negative LW feedback of around 2.0 W m^{-2} K^{-1} each (Fig. 6). Soden et al. (2004) point out that this feedback is not representative of the actual cloud feedback term. However, we are still able to compare it to similar diagnostics from other models. One model out of the 10 models presented in Fig. 7.2 of the 2001 Intergovernmental Panel on Climate Change (IPCC) report had a similar cloud radiative forcing feedback (Houghton et al. 2001); other models behaved quite differently. As the clear-sky Y values from the scanner data (Fig. 6) resemble the total Y values for the Pinatubo response (Fig. 4), it is interesting to speculate that this may indicate that Pinatubo caused few cloud changes.

8. Conclusions

Data from the ERBS instruments appear sufficiently well calibrated to estimate the climate feedback parameter. Using the best estimate of radiative forcing and the GISS surface temperature dataset, a value for the climate feedback parameter is particularly well determined in the LW for 1985–90, where Y_{LW} is 3.7 ± 0.9 W m^{-2} K^{-1}. Overall, for 1985–96 the ERBE data suggest that Y_{NET} is 2.3 ± 1.3 W m^{-2} K^{-1} (Fig. 4). This indicates a net positive feedback, compared to the blackbody response. Uncertainties in specifying surface temperature and radiative forcing changes are examined and found to be a smaller source of error than quoted uncertainties in the regression analyses. Forcing uncertainty is estimated to vary Y_{NET} by no more than ~0.5 W m^{-2} K^{-1}, and surface temperature change uncertainty varies Y_{NET} by ~0.2 W m^{-2} K^{-1}. Our data gave an overall uncertainty range for Y_{NET} of 2.3 ± 1.4 W m^{-2} K^{-1} (not accounting for uncertainty in the ERBE time series, N).

Our results show a net positive feedback relative to the blackbody response, which is consistent with climate models; they also hint at the possibility of near-neutral longwave feedback, which is inconsistent with most (if not all) climate models (Houghton et al. 2001; Colman 2003). However, as our longwave results are only well constrained for the 1985–90 period, it is probably premature to conclude that climate models are incorrectly modeling longwave feedbacks.

These results indicate a 1.0–4.1-K range warming for a doubling of CO_2 (assuming Gaussian-distributed errors in the observable parameters and a radiative forcing for a doubling of CO_2 of 3.7 W m^{-2}). Several state-of-the-art climate models exhibit climate sensitivities closer to the upper bound (Houghton et al. 2001), which would imply a Y_{NET} = 1.0 W m^{-2} K^{-1}. Simply inspecting the range of variations in N and ΔT_s in the figures shows that this value is extremely unlikely. It was noticed that climate models underestimate the ERBE decadal variability (Wielicki et al. 2002) in N. Even though this conclusion was based on data from the uncorrected ERBE analysis, our results suggest that this underestimate in variability could be because climate models tend to overestimate the equilibrium climate sensitivity. A climate model with a smaller sensi-

tivity would produce larger variability in N, for the same variability in ΔT_s.

Patterns of surface and vertical temperature change and Hadley Centre model results indicate that the Y values found for the ERBE record are likely to be representative of that associated with longer-term climate change scenarios and the equilibrium climate sensitivity. The climate feedback from Mt. Pinatubo time period appears to be different. This means that the Y values derived may not necessarily be applicable to all forcing mechanisms, but it could also mean that short time-scale variability has different feedback properties.

The ERBE scanner record, although it only covers 5 yr, gives some intriguing, but somewhat uncertain, insights into the different components of the climate feedback parameter. In particular, it suggests a near-neutral cloud feedback (by offsetting a negative LW cloud feedback against a positive SW cloud feedback). It also suggests a positive surface albedo feedback. The scanning data show the potential benefits that could arise from 10 or more years of well-calibrated data of this kind.

We believe we have illustrated a powerful technique for determining linear components of climate feedback. Until now, it has been very difficult to assess how realistic a given climate model's feedback is, as we lacked measures of distinguishing a "good" model from a "bad." Comparing these ERBE analyses with those from climate models would facilitate such judgments.

Acknowledgments. R. Allan and T. M. Wong are thanked for providing the ERBE data; G. Stenchikov, L. Oman, M. Sato, and G. Myhre are thanked for proving radiative forcing data. PMF would like to thank Martin Manning, Susan Solomon, Keith Shine, Myles Allen, and the MSc climate change class of 2004 for useful discussion and funding from a NERC Advanced Research Fellowship. Work at the Hadley Centre was supported by the U.K. Department for Environment, Food and Rural Affairs under Contract PECD 7/12/37 and by the Government Meteorological Research and Development Programme.

APPENDIX

Linear Regression and Its Uncertainty

A "robust" technique was used to estimate the errors in our regression analysis. As our datasets are relatively short, robust techniques give a truer estimate of the likely errors (Feigelson and Babu 1992). We generated 10 000 Monte Carlo simulations, subsetting an equal number of random data points from the original dataset, and performing OLS regression for each of these sets. The quoted mean and 95% uncertainty in Y is then derived from the mean and standard deviation of the 10 000 simulated Y values.

The appropriate choice of regression analysis is complicated by the fact that we are unable to determine the error characteristics of $Q-N$ and ΔT_s. An accurate estimate of Y will likely not result even with perfect data, because of unknown intrinsic variations in N or ΔT_s, which do not fit the simple linear model. For less than perfectly correlated data, OLS regression of $Q-N$ against ΔT_s will tend to underestimate Y values and therefore overestimate the equilibrium climate sensitivity (see Isobe et al. 1990). However, for a couple of reasons, we believe OLS regression gave a better estimate of climate sensitivity than other approaches examined:

1) The OLS regression model of y against x assumes no "error" in x. Although we cannot characterize the intrinsic independent variations, or errors, in either $Q-N$ or ΔT_s, we imagine several types of cloud changes could cause $Q-N$ to vary independently of global-mean surface temperature. It is more difficult to imagine a change in ΔT_s that N does not respond to. Isobe et al. (1990) recommend the use of OLS when variation x is the cause of variation in y, which we believe is mostly the case with our data.
2) OLS regression of $Q-N$ against ΔT_s was found to be the best predictor of the climate sensitivity in the Hadley Centre climate model. Values of Y derived from short 10-yr time series agreed best with the value derived from longer-term datasets (and the climate sensitivity to $2 \times CO_2$) when OLS regression of $Q-N$ of ΔT_s was used. For example, the OLS bisector method applied to HadCM3 simulations of the observational period gave $Y = 2.9 \pm 0.7$ W m^{-2} K^{-1}, a range that does not include the true value for HadCM3 projections.

Another important reason for adopting our regression model was to reinforce the main conclusion of the paper: the suggestion of a relatively small equilibrium climate sensitivity. To show the robustness of this conclusion, we deliberately adopted the regression model that gave the highest climate sensitivity (smallest Y value). It has been suggested that a technique based on total least squares regression or bisector least squares regression gives a better fit, when errors in the data are uncharacterized (Isobe et al. 1990). For example, for 1985–96 both of these methods suggest Y_{NET} of around 3.5 ± 2.0 W m^{-2} K^{-1} (a 0.7–2.4-K equilibrium surface temperature increase for $2 \times CO_2$), and this should be

compared to our 1.0–3.6-K range quoted in the conclusions of the paper.

REFERENCES

Cess, R. D., and Coauthors, 1996: Cloud feedback in atmospheric general circulation models: An update. *J. Geophys. Res.,* **101D,** 12 791–12 794.

Colman, R., 2003: A comparison of climate feedbacks in general circulation models. *Climate Dyn.,* **20,** 865–873.

——, S. B. Power, and B. J. McAvaney, 1997: Non-linear climate feedback analysis in an atmospheric general circulation model. *Climate Dyn.,* **13,** 717–731.

Feigelson, E. D., and G. J. Babu, 1992: Linear-regression in astronomy. 2. *Astrophys. J.,* **397,** 55–67.

Forest, C. E., P. H. Stone, A. P. Sokolov, M. R. Allen, and M. D. Webster, 2002: Quantifying uncertainties in climate system properties with the use of recent climate observations. *Science,* **295,** 113–117.

Forster, P. M. D., and M. Collins, 2004: Quantifying the water vapour feedback associated with post-Pinatubo global cooling. *Climate Dyn.,* **23,** 207–214.

Gregory, J. M., R. J. Stouffer, S. C. B. Raper, P. A. Stott, and N. A. Rayner, 2002: An observationally based estimate of the climate sensitivity. *J. Climate,* **15,** 3117–3121.

——, and Coauthors, 2004: A new method for diagnosing radiative forcing and climate sensitivity. *Geophys. Res. Lett.,* **31,** L03205, doi:10.1029/2003GL018747.

Hall, A., and S. Manabe, 1999: The role of water vapor feedback in unperturbed climate variability and global warming. *J. Climate,* **12,** 2327–2346.

Hansen, J., M. Sato, and R. Ruedy, 1997: Radiative forcing and climate response. *J. Geophys. Res.,* **102** (D6), 6831–6864.

——, R. Ruedy, J. Glascoe, and M. Sato, 1999: GISS analysis of surface temperature change. *J. Geophys. Res.,* **104** (D24), 30 997–31 022.

——, and Coauthors, 2002: Climate forcings in Goddard Institute for Space Studies SI2000 simulations. *J. Geophys. Res.,* **107,** 4347, doi:10.1029/2001JD001143.

Harvey, L. D. D., and R. K. Kaufmann, 2002: Simultaneously constraining climate sensitivity and aerosol radiative forcing. *J. Climate,* **15,** 2837–2861.

Houghton, J. T., G. J. Jenkins, and J. J. Ephraums, Eds., 1990: *Scientific Assessment of Climate Change.* Cambridge University Press, 365 pp.

——, Y. Ding, D. J. Griggs, M. Noguer, P. J. van der Linden, X. Dai, K. Maskell, and C. A. Johnson, Eds., 2001: *Climate Change 2001: The Scientific Basis.* Cambridge University Press, 881 pp.

Isobe, T., E. D. Feigelson, M. G. Akritas, and G. J. Babu, 1990: Linear-regression in astronomy. 1. *Astrophys. J.,* **364,** 104–113.

Jacobowitz, H., H. V. Soule, H. L. Kyle, and F. B. House, 1984: The Earth Radiation Budget (Erb) Experiment—An overview. *J. Geophys. Res.,* **89D,** 5021–5038.

Jones, P. D., M. New, D. E. Parker, S. Martin, and I. G. Rigor, 1999: Surface air temperature and its changes over the past 150 years. *Rev. Geophys.,* **37,** 173–199.

Joshi, M., K. Shine, M. Ponater, N. Stuber, R. Sausen, and L. Li, 2003: A comparison of climate response to different radiative forcings in three general circulation models: Towards an improved metric of climate change. *Climate Dyn.,* **20,** 843–854.

Knutti, R., T. F. Stocker, F. Joos, and G. K. Plattner, 2003: Probabilistic climate change projections using neural networks. *Climate Dyn.,* **21,** 257–272.

Leggett, J. A., W. J. Pepper, and R. J. Swart, 1992: Emmissions scenarios for the IPCC: An update. *Climate Change 1992: The Supplemenatary Report to the IPCC Scientific Assessment,* J. T. Houghton, B. A. Callander, and S. K. Varney, Eds., Cambridge University Press, 69–95.

Levitus, S., J. I. Antonov, T. P. Boyer, and C. Stephens, 2000: Warming of the world ocean. *Science,* **287,** 2225–2229.

Myhre, G., A. Myhre, and F. Stordal, 2001: Historical evolution of radiative forcing of climate. *Atmos. Environ.,* **35,** 2361–2373.

Sato, M., J. E. Hansen, M. P. McCormick, and J. B. Pollack, 1993: Stratospheric aerosol optical depths, 1850–1990. *J. Geophys. Res.,* **98** (D12), 22 987–22 994.

Senior, C. A., and J. F. B. Mitchell, 2000: The time-dependence of climate sensitivity. *Geophys. Res. Lett.,* **27,** 2685–2688.

Soden, B. J., 1997: Variations in the tropical greenhouse effect during El Niño. *J. Climate,* **10,** 1050–1055.

——, R. T. Wetherald, G. L. Stenchikov, and A. Robock, 2002: Global cooling after the eruption of Mount Pinatubo: A test of climate feedback by water vapor. *Science,* **296,** 727–730.

——, A. J. Broccoli, and R. S. Hemler, 2004: On the use of cloud forcing to estimate cloud feedback. *J. Climate,* **17,** 3661–3665.

Stott, P. A., S. F. B. Tett, G. S. Jones, M. R. Allen, J. F. B. Mitchell, and G. J. Jenkins, 2000: External control of 20th century temperature by natural and anthropogenic forcings. *Science,* **290,** 2133–2137.

Wielicki, B. A., and Coauthors, 2002: Evidence for large decadal variability in the tropical mean radiative energy budget. *Science,* **295,** 841–844.

Zhang, Y. C., W. B. Rossow, A. A. Lacis, V. Oinas, and M. I. Mishchenko, 2004: Calculation of radiative fluxes from the surface to top of atmosphere based on ISCCP and other global data sets: Refinements of the radiative transfer model and the input data. *J. Geophys. Res.,* **109,** D19105, doi:10.1029/2003JD004457.